Supplementary Information

Supplementary Figures and legends.

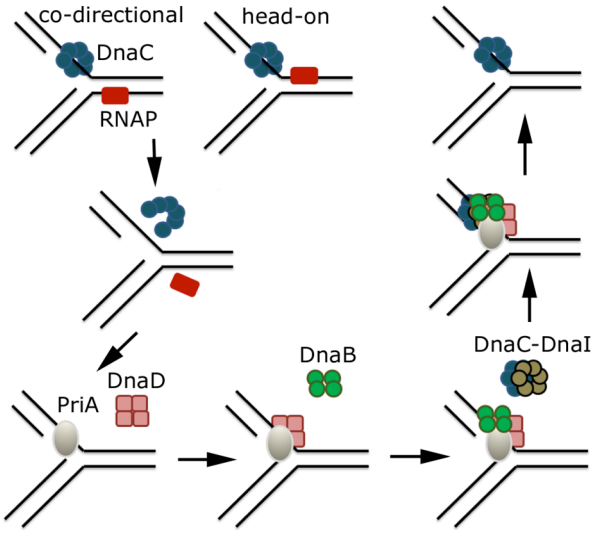

Supplementary Fig. 1. A simple model for PriA-mediated resolution of replication-transcription conflicts. Co-directional and head-on collisions with RNAP at highly transcribed regions cause replication fork collapse and disengagement of the helicase DnaC to vacate a small single stranded region on the lagging strand. PriA binds strongly to this forked substrate and sequentially recruits DnaD and DnaB[35]. DnaC (helicase) is then reloaded onto the lagging strand from its complex with the AAA+ loader protein DnaI.

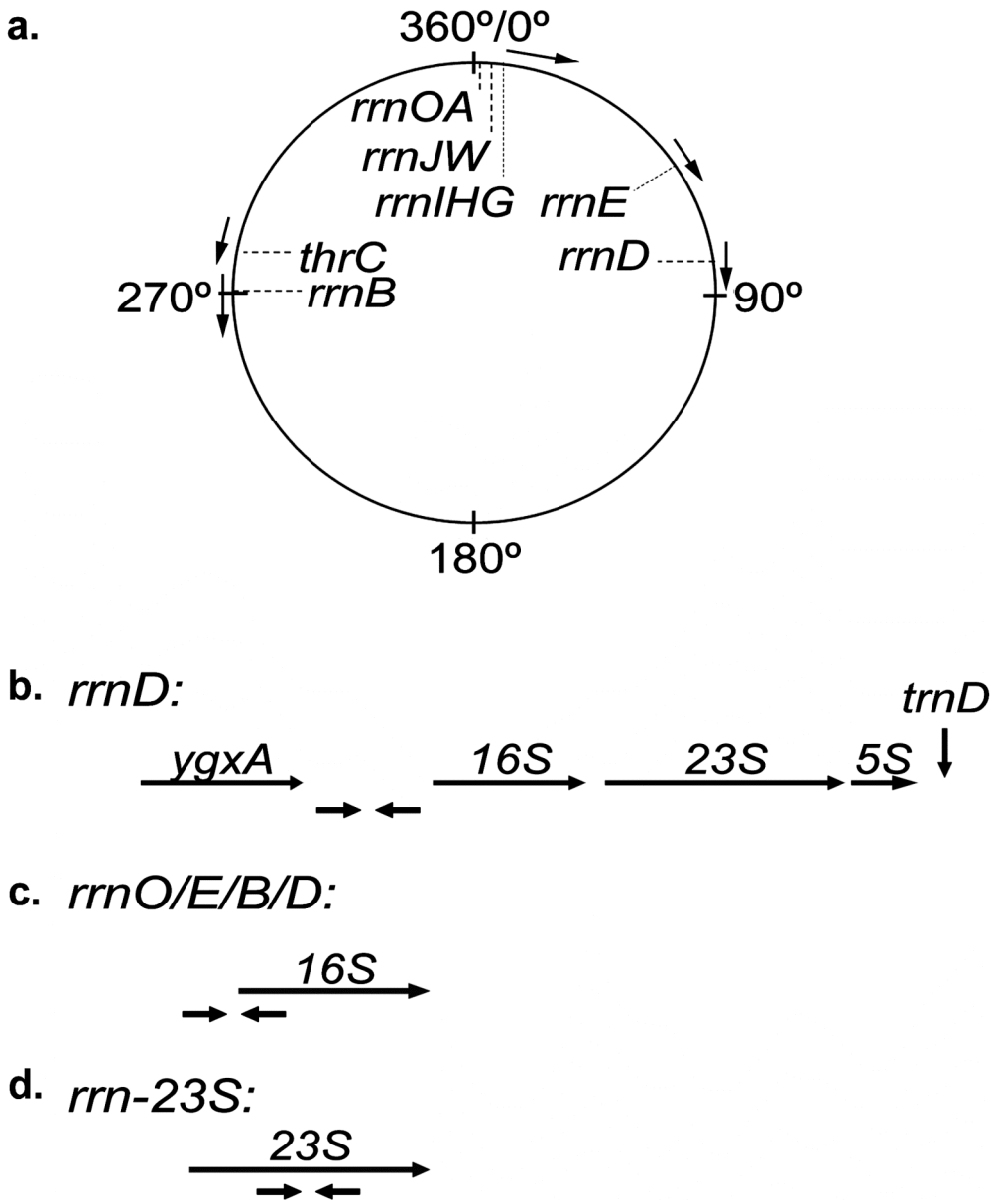

Supplementary Fig. 2. Map of *B. subtlis* chromosome with *rrn* genes and cartoon of primers used. **a.** Circular map of the *B. subtilis* chromosome. The origin of replication (*oriC*) is at 0°/360°. rRNA genes (*rrn*) are shown and are all co-directional with replication. *thrC* (co-directional to replication) is the site of integration of the Pxis-*lacZ* fusion that is head-on with replication. **b-d.** Cartoons of *rrn* loci and the primers used for qPCR. **b.** *rrnD*. Primers amplify a region upstream of and unique to *rrnD*. **C.** Primers amplify a region extending from upstream of and extending into the 16S rRNA genes from *rrnO*, *E*, *B*, *D*. **d.** Primers amplify a region internal to all 23S rRNA genes.

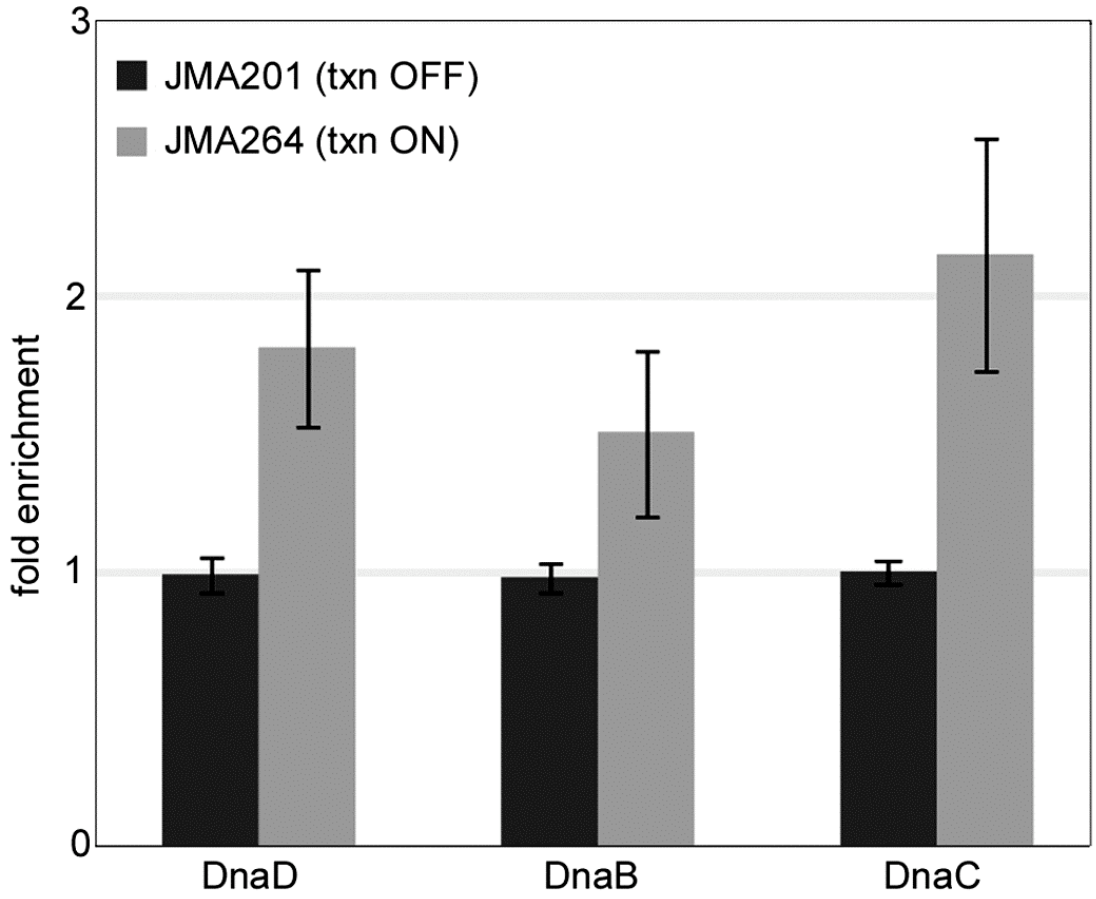

Supplementary Fig. 3. Increased association of DnaD, DnaB, and helicase (DnaC) during head-on conflicts between transcription and replication. Association of DnaD, DnaB, and helicase was measured by ChIP-qPCR in strains with Pxis-*lacZ* inserted at *thrC* in the head-on orientation[36]. Strain JMA264 (gray bars) is missing ICE*Bs1* and its repressor, and Pxis-*lacZ* is on. Strain JMA201 (black bars) contains ICE*Bs1*, expresses the repressor, and Pxis-*lacZ* is off.

Primers used to detect DNA from the *thrC* region were: HM120 - 5'-GATGAATGCACGCTGAACG-3' and HM121 - 5'-GTTTGCAGCGGTTCAGAC-3' and amplify DNA from *yutG*, the gene just before the transcription terminator in the operon.

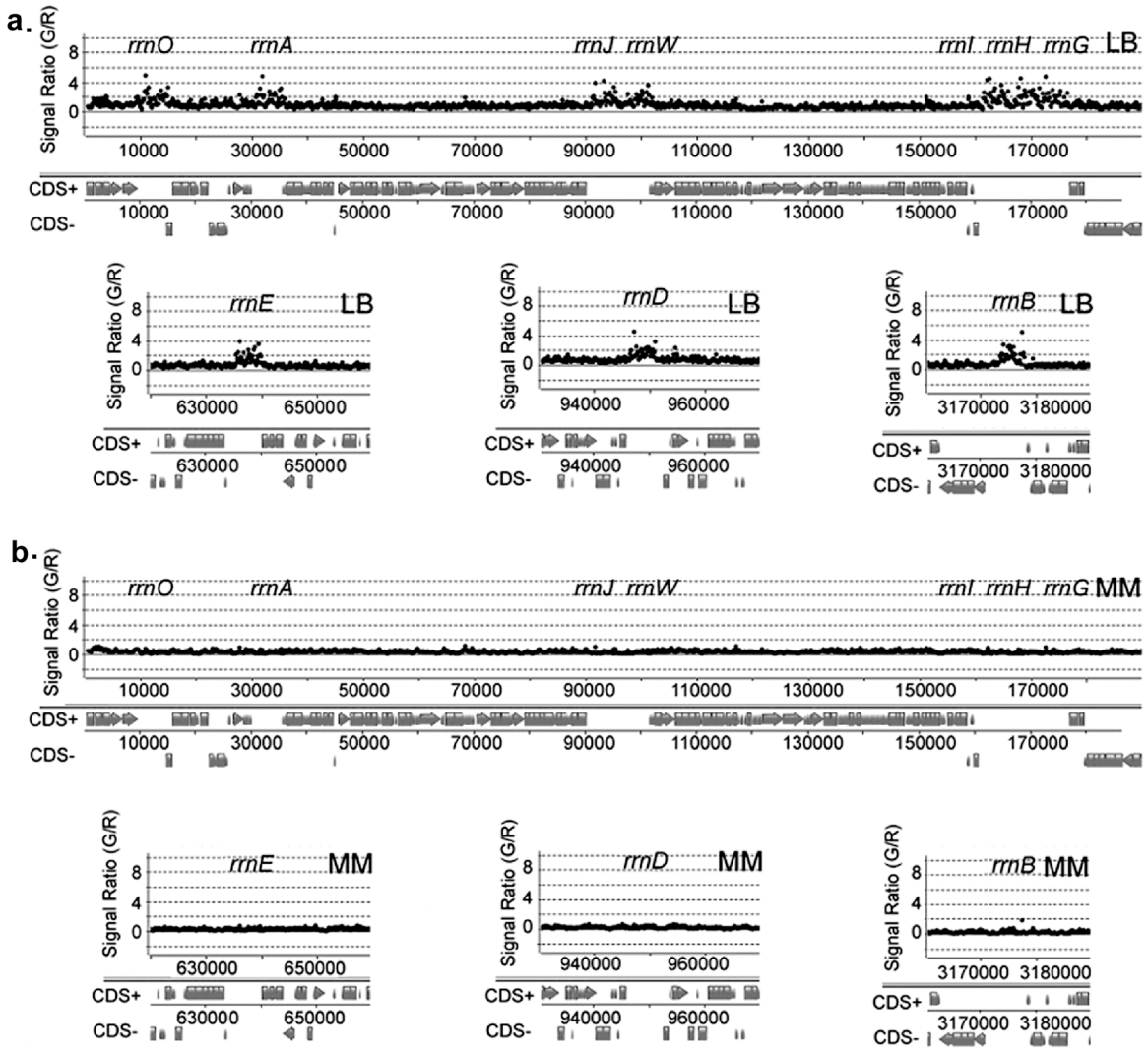

Supplementary Fig. 4. ChIP-chip analysis of DnaD. Wild type cells (strain 168) were grown in LB (**a**) or LeMaster minimal medium (**b**) and sampled during exponential growth. Data are plotted as in Fig. 1 and Fig. 2 (main text). The chromosomal positions are shown from 0 kb (*oriC*) to just past *rrnI*, *H*, *G* at ~200 kb and the other *rrn* regions are in separate panels.

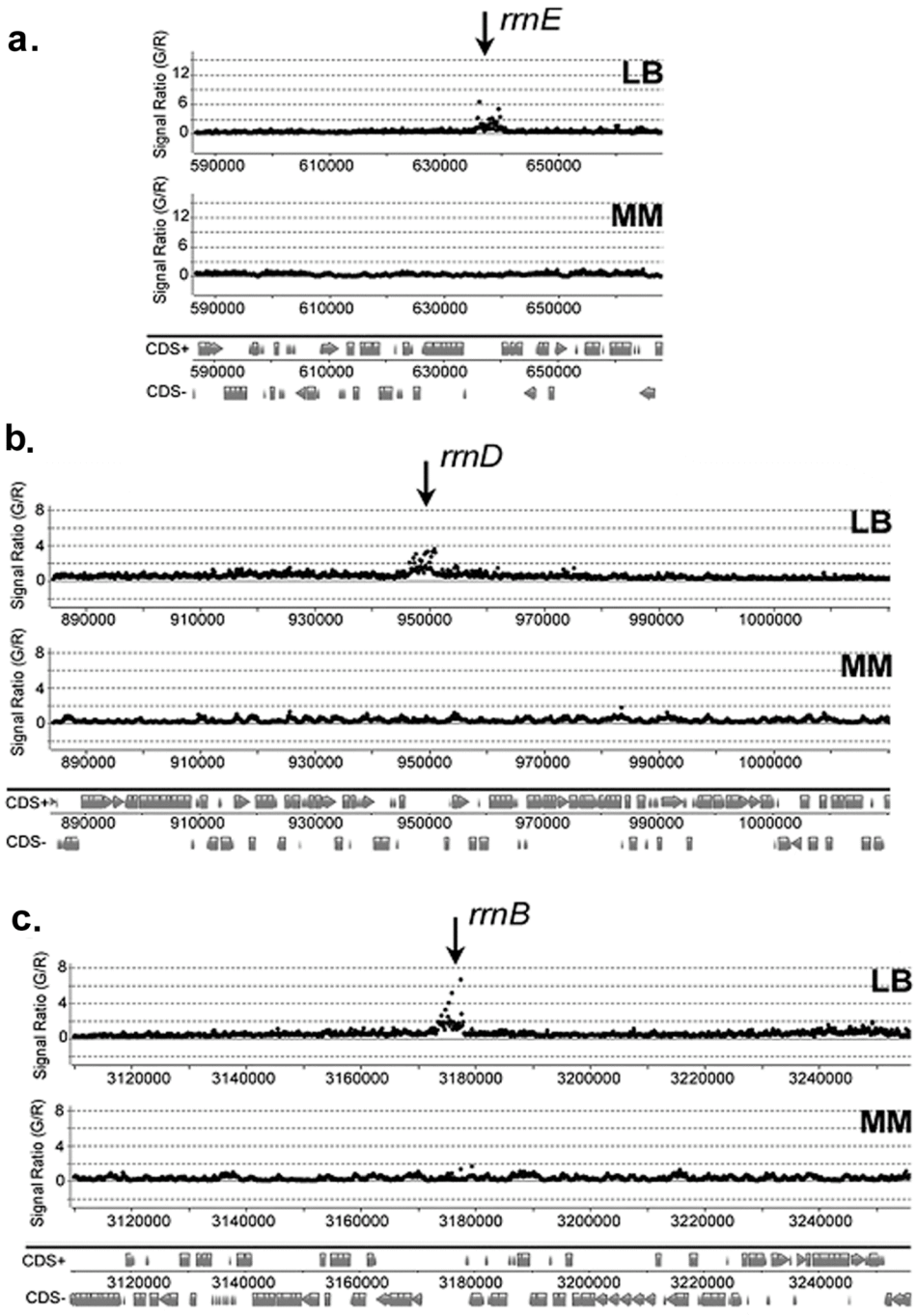

Supplementary Fig. 5. ChIP-chip analysis of DnaB. Data are from the same experiment as in Fig. 2 (main text) from cells grown in rich (LB) medium and minimal medium (MM). **a.** *rrnE*. **b.** *rrnD*. **c.** *rrnB*.

Supplementary Table. *B. subtilis* strains.

Strain	Genotype; comment
168	*trpC2*; wild type
AG174	*trpC2 pheA1*; wild type
AIG200	Δ*dnaA-oriC-dnaN*::*spc*, *amyE*::pMMB26(P_{xylA}-*dnaN*, *cat*), *spoIIIJ*::pMMB138(*oriN*, *kan*), *pheA1*, *trpC*+; *dnaA* null mutant[37,38]
JMA201	*thrC*::(Pxis-*lacZ erm*) ICE*Bs1*$^{+}$ *pheA1*, *trpC2*; Pxis is OFF due to presence of ICE*Bs1* and production of the repressor ImmR[36]
JMA264	*thrC*::(Pxis-*lacZ erm*) ICE*Bs1*^{0} *pheA1*, *trpC2*; Pxis is ON due to absence of ICE*Bs1* (no ImmR)[36]
WKS338	*amyE*::{Pspank(-*7TA*)-*sspB*, *spc*}, *priA*::pGCS-priA (*cat*) {*priA-ssrA**}

Supplementary Discussion

DnaB ChIP-chip experiments. Two independent analyses of ChIP-chip data for DnaB are presented elsewhere. In one case, data are presented in the context of DnaB function at *oriC* and use the same microarrays as presented here[39]. In the second case, both DnaD and DnaB were analyzed using microarrays containing probes corresponding to all (or most) annotated open reading frames and many intergenic regions[40], but did not contain rRNA gene probes[41]. DnaB is associated with the *oriC* and *terC* regions. In addition, both DnaD and DnaB are associated with chromosomal regions bound by DnaA, and this association depends on *dnaA*[41].

Association of helicase with *rrn* loci is independent of the replication initiator DnaA and replication initiation from *oriC*. DnaD and DnaB (and DnaI) assemble helicase during replication initiation at *oriC*. This assembly depends on the replication initiator DnaA[42]. We

found that association of helicase at the *rrn* loci was independent of DnaA and replication initiation from *oriC*. *B. subtilis oriC* and *dnaA* are dispensable in strains with a heterologous origin of replication inserted elsewhere in the chromosome[43]. Replication from the heterologous origin *oriN* requires its cognate initiator protein, RepN, and is independent of DnaA[43], but still depends on the other replication initiation proteins. Using strains containing *oriN* and *repN*, inserted at *spoIIIJ*, near *oriC* so that transcription and replication of all *rrn* operons would remain co-directional, a null mutation in *dnaA*, and a non-functional *oriC*[38], we found that the replicative helicase was associated with the *rrn* loci (Fig. 4), although the association was less than that observed when replication initiated from *oriC*. This difference is likely due to less frequent replication initiation from *oriN* than from *oriC* during rapid growth, causing under-replication in the *oriN* strains[44]. From these results, we conclude that association of helicase with rRNA regions is independent of DnaA and replication initiation from *oriC*.

Estimate of the number of RNAP molecules per rRNA operon in *B. subtilis*. We estimated the average number of RNAP molecules per *rrn* operon in two ways: 1) by direct analogy to *E. coli* where there are very good numbers based on direct electron micrographic (EM) visualization[45]; and 2) by rough calculations based on the number of ribosomes per cell determined for *B. licheniformis*[46], a close relative of *B. subtilis*.

The average number of RNAP molecules per rRNA operon in *E. coli* growing rapidly in rich medium is approximately 50-55, as determined in electron micrographs[45]. Assuming that the efficiency of production and processing of rRNA is comparable in *E. coli* and *B. subtilis*, *B. subtilis* likely has more ribosomes per cell than *E. coli* since its cells are larger. There are seven *rrn* operons in *E. coli*, compared to ten in *B. subtilis*. If *B. subtilis* and *E. coli* have the same number of ribosomes per cell at rapid growth rates (20 min doubling time), then we estimate that

there would be 35-40 RNAP molecules per *rrn* operon in *B. subtilis*. This is almost certainly an underestimate.

We also estimated the number of RNAP molecules per rRNA operon in *B. subtilis* based on measurements of the number of ribosomes per cell in *B. licheniformis* and making several approximations. There are ~92,000 ribosomes per cell in *B. licheniformis* growing with a doubling time of 35 min[46]. *B. subtilis* cells growing in rich medium (LB) with a doubling time of ~20 min most likely have >92,000 ribosomes per cell. We will use 100,000 as an estimate. Since cells were growing rapidly, there were probably 8 copies of the *oriC* region per cell. There are 7 *rrn* operons in the *oriC* region (Fig. S1), so we estimate that there are ~56 copies of *rrn* operons from the *oriC* region per cell, plus probably 2-4 copies of each of the other 3 *rrn* operons, giving an estimate of ~60-70 *rrn* operons per cell. There would need to be ~1,500 transcripts of each operon per cell per 20 min (~75 per min) to produce ~100,000 rRNA molecules per 20 min doubling. If the rate of transcription is ~50 nucleotides/sec (3,000 nucleotides/min) and each *rrn* operon is ~4.5 kb, then it takes ~1.5 min to make a single rRNA from a single operon and there would need to be >100 RNAP molecules (~1.5 x ~75) on average per *rrn* operon.

Mechanism of restart at replication-transcription conflict sites. Replication conflicts are resolved through different mechanisms, some requiring recombination and some operating directly at the sites of conflict[47]. Replication stalling and/or collapse upon encountering DNA lesions require either recombination or fork regression to repair or bypass the lesion. However, replication stalling and/or collapse at sites of conflict with transcription should not be as challenging to resolve because they should not require repair of the DNA substrate. Thus, recombination might be redundant at such sites. Disengagement of the helicase from the lagging

strand upon conflicts with the RNAP will expose a single stranded region on the lagging strand next to the junction where the helicase was bound. PriA can form a specific complex with this type of forked substrate, and this PriA-DNA complex should then induce the sequential recruitment of the helicase loader proteins DnaD and DnaB[35]. Since the 3'-5' helicase activity of PriA is dispensable for replisome assembly[48,49] the simplest model for reloading the helicase is shown in Supplementary Fig. 1.

Supplementary Notes

35. Marsin, S., McGovern, S., Ehrlich, S. D., Bruand, C. & Polard, P. Early steps of *Bacillus subtilis* primosome assembly. *J Biol Chem* **276**, 45818-45825 (2001)
36. Auchtung, J. M., Lee, C. A., Garrison, K. L. & Grossman, A. D. Identification and characterization of the immunity repressor (ImmR) that controls the mobile genetic element ICE*Bs1* of *Bacillus subtilis*. *Mol Microbiol* **64**, 1515-1528 (2007)
37. Goranov, A. I., Katz, L., Breier, A. M., Burge, C. B. & Grossman, A. D. A transcriptional response to replication status mediated by the conserved bacterial replication protein DnaA. *Proc Natl Acad Sci U S A* **102**, 12932-12937 (2005)
38. Berkmen, M. B. & Grossman, A. D. Subcellular positioning of the origin region of the *Bacillus subtilis* chromosome is independent of sequences within *oriC*, the site of replication initiation, and the replication initiator DnaA. *Mol Microbiol* **63**, 150-165 (2007)
39. Grainger, W. H., Machon, C., Scott, D. J. & Soultanas, P. DnaB proteolysis in vivo regulates oligomerization and its localization at *oriC* in *Bacillus subtilis*. *Nucleic Acids Res* **38**, 2851-2864 (2010)
40. Breier, A. M. & Grossman, A. D. Dynamic association of the replication initiator and transcription factor DnaA with the *Bacillus subtilis* chromosome during replication stress. *J Bacteriol* **191**, 486-493 (2009)
41. Smits, W. K., Merrikh, H., Bonilla, C. Y. & Grossman, A. D. Primosomal proteins DnaD and DnaB are recruited to chromosomal regions bound by DnaA in *Bacillus subtilis*. *J. Bacteriol.* (accepted for publication)
42. Smits, W. K., Goranov, A. I. & Grossman, A. D. Ordered association of helicase loader proteins with the *Bacillus subtilis* origin of replication in vivo. *Mol Microbiol* **75**, 452-461 (2010)
43. Hassan, A. K. *et al.* Suppression of initiation defects of chromosome replication in *Bacillus subtilis dnaA* and *oriC*-deleted mutants by integration of a plasmid replicon into the chromosomes. *J Bacteriol* **179**, 2494-2502 (1997)
44. Kadoya, R., Hassan, A. K., Kasahara, Y., Ogasawara, N. & Moriya, S. Two separate DNA sequences within *oriC* participate in accurate chromosome segregation in *Bacillus subtilis*. *Mol Microbiol* **45**, 73-87 (2002)

45. Condon, C., French, S., Squires, C. & Squires, C. L. Depletion of functional ribosomal RNA operons in *Escherichia coli* causes increased expression of the remaining intact copies. *Embo J* **12**, 4305-4315 (1993)
46. van Dijk-Salkinoja, M. S. & Planta, R. J. Rate of ribosome production in *Bacillus licheniformis*. *J Bacteriol* **105**, 20-27 (1971)
47. Heller, R. C. & Marians, K. J. Replisome assembly and the direct restart of stalled replication forks. *Nat Rev Mol Cell Biol* **7**, 932-943 (2006)
48. Liu, J. & Marians, K. J. PriA-directed assembly of a primosome on D loop DNA. *J Biol Chem* **274**, 25033-25041 (1999)
49. Zavitz, K. H. & Marians, K. J. ATPase-deficient mutants of the *Escherichia coli* DNA replication protein PriA are capable of catalyzing the assembly of active primosomes. *J Biol Chem* **267**, 6933-6940 (1992)